Biochemical Pharmacology, Vol. 45, No. 12, pp. 2449–2456, 1993.
Printed in Great Britain.

0006-2952/93 $6.00 + 0.00
Pergamon Press Ltd

DUAL INHIBITION OF TOPOISOMERASE II AND TUBULIN POLYMERIZATION BY AZATOXIN, A NOVEL CYTOTOXIC AGENT

ERIC SOLARY,* FRANÇOIS LETEURTRE, KENNETH D. PAULL,† DOMINIC SCUDIERO,‡ ERNEST HAMEL and YVES POMMIER§

Laboratory of Molecular Pharmacology, Developmental Therapeutics Program, Division of Cancer Treatment, and National Cancer Institute, National Institutes of Health, Bethesda, MD 20892, U.S.A.

(*Received* 14 *December* 1992; *accepted* 23 *February* 1993)

Abstract—Azatoxin (NSC 640737) is a synthetic molecule that was rationally designed as a topoisomerase II inhibitor (Leteurtre *et al.*, *Cancer Res* **52**: 4478–4483, 1992). The present study was undertaken in order to investigate the molecular pharmacology and the cytotoxic activity of azatoxin in human tumor cells. Alkaline elution experiments performed in HL-60 cells demonstrated that: (1) azatoxin induces DNA–protein cross-links and protein-linked DNA single- and double-strand breaks characteristic of topoisomerase II inhibition in HL-60 cells; and (2) the potency of azatoxin is comparable to that of etoposide (VP-16). Testing of azatoxin in 45 human cell lines in the National Cancer Institute (NCI) *in vitro* Drug Screening Program indicated that azatoxin was potent (mean IC_{50} = 0.13 μM), but that its cell line sensitivity profile was correlated with that of tubule inhibitors rather than that of topoisomerase II inhibitors. These data led us to investigate the anti-tubulin activity of azatoxin. We found that azatoxin inhibited tubulin polymerization *in vitro* and was a mitotic inhibitor at 1 μM and above in the human colon cancer cell line KM20L2. In these cells topoisomerase II inhibition, as detected by the induction of protein-linked DNA strand breaks, required azatoxin concentrations of at least 10 μM. In summary, azatoxin is a potent cytotoxic agent that inhibited both tubulin and topoisomerase II. At lower azatoxin concentrations the former activity prevailed whereas at higher concentrations topoisomerase II inhibition became prominent.

Azatoxin (NSC 640737) (Fig. 1) was rationally designed as a topoisomerase II (top2‖) inhibitor by using molecular modeling of pre-existing top2 inhibitors [1, 2]. Using purified top2, we have shown previously that azatoxin is a non-intercalator that induces top2-linked DNA breaks (cleavable complexes) with a unique DNA sequence selectivity [2].

The present study investigated the cellular effects of azatoxin, including DNA damage, tubulin inhibition, cell cycle analysis, and cytotoxicity. Azatoxin was found to produce protein-linked DNA single- and double-strand breaks, as expected for top2 inhibition [3, 4]. Differential cytotoxicity data obtained in the new NCI Drug Screening Program, however, suggested an anti-tubulin activity [5]. This was confirmed by the measurement of the mitotic index of cultured cells and by demonstration of inhibition of tubulin polymerization. Thus, azatoxin is a novel chemical structure that inhibits both tubulin and top2.

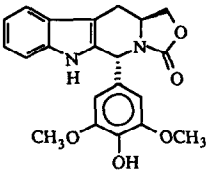

Fig. 1. Structure of azatoxin.

MATERIALS AND METHODS

Cell culture, labeling and drug treatments. Human promyelocytic leukemia HL-60 cells were a gift from Dr. T. Breitman (NCI, Bethesda, MD), and human colon carcinoma cells KM20L2 were obtained from the *in vitro* National Cancer Institute Screening Program. Cells were grown in RPMI-1640 medium supplemented with 10% (v/v) heat-inactivated fetal bovine serum and 2 mM L-glutamine. They were passed twice a week and studied between passages

* Present address: Department of Haematology, University-Hospital, BP 1542, 21034 Dijon Cedex, France.

† Present affiliation: Information Technology Branch, Developmental Therapeutics Program, Division of Cancer Treatment, Executive Plaza North, Bethesda, MD.

‡ Permanent affiliation: Program Resources, Incorporated/Dynacorp, National Cancer Institute, Frederick Cancer Research and Development Center, Box B, Frederick, MD 21702.

§ Corresponding author: Dr Yves Pommier, Bldg. 37, Rm. 5C25, National Cancer Institute, NIH, Bethesda, MD 20892. Tel. (301) 496-5944; FAX (301) 402-0752.

‖ Abbreviations: DPC, DNA–protein cross-links; DSB, DNA double-strand breaks; GI_{50}, growth inhibitory 50% concentration; HBSS, Hanks' balanced salt solution; PBS, phosphate-buffered saline; SDS, sodium dodecyl sulfate; SSB, DNA single-strand breaks; TCA, trichloroacetic acid; top2, DNA topoisomerase II; and VP-16, etoposide.

20 and 40. Chinese hamster lung fibroblasts DC3F, used as internal standard cells in alkaline elution, were grown in Eagle's modified minimum essential medium supplemented with 10% (v/v) heat-inactivated fetal bovine serum, 2 mM L-glutamine, 1 mM sodium pyruvate and 0.1 mM non-essential amino acids. Cells were grown at 37° in an atmosphere of 95% air and 5% CO_2. All cell culture products were purchased from Advanced Biotechnologies Inc. (Columbia, MD) and routinely monitored for the absence of *Mycoplasma* contamination.

Azatoxin was synthesized at the Department of Chemistry, University of Virginia, Charlottesville, VA, by the method of Tomioka *et al.* [6]. Etoposide (VP-16) was obtained from the Bristol-Myers-Squibb Co., Wallingford, CT. Drug stock solutions were made in dimethyl sulfoxide at 10 mM. Further dilutions were made in distilled water. The final concentration of dimethyl sulfoxide in culture medium did not exceed 1% (v/v), and this was non-toxic to the cells.

[*methyl*-^{3}H]Thymidine (78.5 Ci/mmol) and [2-^{14}C]-thymidine (59 mCi/mmol) were purchased from New England Nuclear (Boston, MA). All other chemicals, including non-radiolabeled thymidine, were reagent grade.

DNA damage measurements using alkaline elution. DNA damage was quantitated by alkaline elution filter methods, as described by Kohn *et al.* [7, 8]. Briefly, HL-60 cell labeling was performed by adding 0.1 μCi/mL of [*methyl*-^{3}H]thymidine or 0.02 μCi/mL of [2-^{14}C]thymidine for 1.5 to 2 doubling times to exponentially growing cells seeded at an initial cell concentration of 5×10^5/mL. Cells were chased in isotope-free medium overnight and treated with drugs for the indicated times. To measure the production of DNA lesions produced by azatoxin and VP-16, cells were washed in 10 mL of ice-cold Hanks' balanced salt solution (HBSS, Quality Biological Inc., Gaithersburg, MD), before loading onto the filters as described [9]. To determine the rate of reversal of drug-induced DNA lesions, cells were washed with 5 mL of complete medium twice at 37°, and then further incubated in 5 mL of complete medium before loading onto the filters.

DNA single-strand breaks (SSB). ^{14}C-Labeled drug-treated cells were loaded onto polycarbonate filters (2 μm pore size, 25 mm diameter; Nucleopore Corp., Pleasanton, CA) that had been prewashed with ice-cold HBSS. Cells were lysed in 5 mL of 2% (w/v) sodium dodecyl sulfate (SDS), 0.5 mg/mL of proteinase K (Boehringer Mannheim, Indianapolis, IN) at pH 10. ^{3}H-Labeled DC3F-internal standard cells that had been irradiated on ice with 2000 rads from a ^{137}Cs source were added to the filters in a minimum volume (<0.3 mL) and immediately lysed with 5 mL of lysis solution [2% (w/v) SDS, 0.025 M Na_2 EDTA, 0.1 M glycine, pH 10.0, plus 0.5 mg/mL of proteinase K]. The lysis solution was washed from the filters with 0.02 M EDTA, pH 10 (5 mL), and the DNA was eluted with tetrapropylammonium hydroxide (RSA Corp., Ardsley, NY)/EDTA, pH 12.1, containing 0.1% (w/v) SDS, at a flow rate of 0.08 to 0.12 mL/min. Fractions were collected at 5-min intervals for 30 min. Elution curves were normalized with respect to internal standard cells in order to compensate for differences in flow rates between individual elution samples. SSB frequency expressed in rad-equivalents was calculated from the formula:

$$\mathrm{SSB} = [\log (r_1/r_0)/\log (R_0/r_0)] \times 2000$$

where R_0, r_0 and r_1 are the fractions of [^{14}C]DNA retained on the filter for 2000-rad irradiated control cells, unirradiated control cells, and drug-treated cells, respectively.

DNA double-strand breaks (DSB). Approximately 5×10^5 cells were loaded onto each polycarbonate filter. Elution was performed with tetrapropylammonium hydroxide/EDTA, pH 9.6, containing 0.1% (w/v) SDS, at pH 9.6, layered above 2 mL of lysis solution (same as above). Elution was carried out at a flow rate of 0.03 to 0.04 mL/min for 15 hr, and fractions were collected at 3-hr intervals. Azatoxin and VP-16 gave nearly linear elution curves. The similarity between these curves and those of irradiated cells allowed the expression of the drug-induced DSB in DSB rad equivalents [10].

DNA–protein cross-links (DPC). ^{14}C-Labeled control and drug-treated cells and ^{3}H-labeled DC3F internal standard cells were irradiated on ice with 3000 rads. ^{14}C-Labeled cells were kept on ice and then loaded onto prewashed ice-cold Metricel™ membrane filters (0.8 μm pore size, 25 mm diameter; Gelman Sciences Inc., Ann Arbor, MI), and lysed with 5 mL of 2% (w/v) SDS, pH 10 [7]. Irradiated ^{3}H-labeled internal standard cells were added to the filters in a minimum volume (<0.3 mL) and immediately lysed with 5 mL of 2% (w/v) SDS. The lysis solution was washed from the filters with 0.02 M EDTA, pH 10 (5 mL), and the DNA eluted from the filters overnight with tetrapropylammonium hydroxide/EDTA, pH 12.1, without SDS, at a flow rate of 0.02 to 0.03 mL/min. DPC were quantitated using the bound-to-one-terminus model [7] from the formula:

$$\mathrm{DPC} = [(1 - R_1)^{-1} - (1 - R_0)^{-1}] \times 3000$$

where R_1 and R_0 are the fractions of [^{14}C]DNA remaining on the filter for drug-treated and untreated cells, respectively. DPC were expressed in rad-equivalents.

NCI drug screening assays. The methodology employed by the NCI *in vitro* Drug Screening Program has been discussed in detail [11]. Cell lines were obtained and characterized as described previously [11]. Cellular response to azatoxin was evaluated using a sulforhodamine-B assay. Briefly, the human tumor cell lines making up the screening panel were grown in RPMI-1640 medium containing 5% fetal bovine serum and 2 mM L-glutamine. Cells were inoculated in 100-μL aliquots into 96-well tissue culture plates at appropriate cell densities and incubated at 37° for 24 hr prior to the addition of the drug. Azatoxin was solubilized in dimethyl sulfoxide (DMSO) and added in five sequential 10-fold dilutions with 10^{-4} M being the highest concentration tested. After incubation of the plates at 37° for 48 hr, the remaining cells were fixed with trichloroacetic acid (TCA), stained with 0.04% sulforhodamine-B for 10 min, and washed with 1%

acetic acid to remove excess stain. Protein-bound stain was solubilized in 50 μL Tris buffer, and optical density (O.D.) read in an automated plate reader at 515 nm. Growth inhibition was calculated as the fraction of cell growth relative to control for each cell line from three different O.D. measurements [11]: untreated control (C), drug-treated test O.D. (T), and time 0 O.D. (T_0) (O.D. of untreated cells at time of drug addition).

If $T \geq T_0$, the equation:

$$(T - T_0)/(C - T_0)$$

is used; and

if $T < T_0$, the equation:

$$(T - T_0)/T_0$$

is used.

Colony-formation assay in KM20L2 cells. A fixed number of KM20L2 cells were plated in 25 cm^2 flasks in medium for 24 hr before azatoxin treatment for an additional 24 hr. Cell cultures were washed twice with 10 mL of HBSS (37°), trypsinized, and counted using a Coulter counter (Coulter Electronics Inc., Hialeah, FL) to determine the number of cells that were detached after 24 hr of treatment. Then 10^2, 10^3 and 10^4 adherent cells were plated in triplicate in 25 cm^2 flasks with 5 mL of fresh medium. Colonies were grown for 10–12 days. Culture flasks were then washed with ice-cold phosphate-buffered saline (PBS), fixed with methanol (95%), and stained with methylene blue (0.05%) [12]. Results are expressed as log of survival fraction that was calculated by dividing the number of colonies in treated flasks by those of control flasks.

Cell cycle analysis and mitotic index determinations. After drug treatment, HL-60 cells and trypsinized KM20L2 cells were harvested by centrifugation, washed twice in ice-cold PBS, pH 7.5, and incubated on ice for 1 hr in 70% ethanol. Following fixation, cells were washed twice in ice-cold PBS, pH 7.5, and incubated for 1 hr at 25° in PBS containing 500 U/mL of RNase A (Sigma Chemical Co., St. Louis, MO). Cells were washed again in PBS, resuspended, and stored on ice prior to analysis. Cellular DNA was stained with propidium iodide, and cell-cycle determination was performed using a Beckton-Dickinson fluorescence-activated cell analyzer. Data were interpreted using the SFIT model program provided by the manufacturer. Results are expressed as a percentage of total cells at a specific cell phase.

The accumulation of exponentially growing cells in mitosis (mitotic index) was determined after exposure to azatoxin. Cells were washed once with ice-cold PBS, resuspended in 0.5 mL of half-strength PBS for 10 min, and stored for 30 min at 4° after adding 6 mL of a 2% solution of 3:1 ethanol:glacial acetic acid. Samples were resuspended in 0.25 mL of 3:1 ethanol:glacial acetic acid for 10 min, smeared onto glass slides, and stained with Giemsa. The number of cells in mitosis was recorded from random population samplings totaling 500 cells.

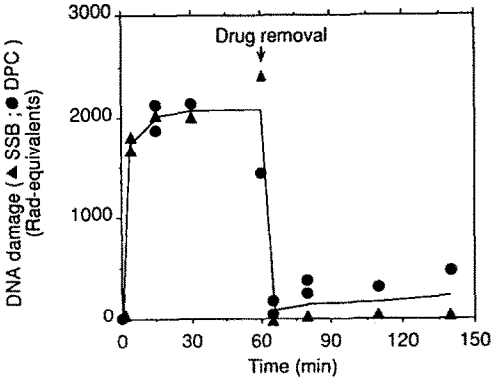

Fig. 2. Kinetics of SSB (▲) and DPC (●) induced by azatoxin. HL-60 cells were treated at time 0 with 20 μM azatoxin. Azatoxin was removed from the culture medium after 60 min by centrifugation and resuspension in drug-free medium at 37°. At the indicated times, DNA damage was assayed by alkaline elution. Each point represents an independent determination.

Tubulin polymerization inhibition assays. Assays were performed as described previously [13]. Reaction mixtures contained in a 0.25-mL final volume 0.25 mg of electrophoretically homogeneous bovine brain tubulin (10 μM) [14], 1.0 M magnesium-free monosodium glutamate, pH 6.6 [15], 0.25 mM $MgCl_2$, 4% (v/v) dimethyl sulfoxide, 0.4 mM GTP, and various concentrations of azatoxin. All components except GTP were incubated at 30° for 15 min in 0.24 mL and chilled on ice. GTP, required for tubulin polymerization, was added to each sample in 10 μL. Samples were transferred to Gilford 250 and 2400S recording spectrophotometers equipped with electronic temperature controllers. Baselines were established with the cuvettes held at 0°, and reactions were initiated by a temperature jump (about 60 sec) to 30°. Polymerization was followed turbidimetrically for 20 min at 30°. Depolymerization was initiated by cooling samples to 0°. The IC_{50} values, defined as the inhibitor concentration required to suppress the extent of polymerization by 50% after 20 min, were calculated from a sigmoid model with no A_{350} variation and the control's A_{350} variation set at 100 and 0% inhibitory effects, respectively.

RESULTS

Protein-linked SSB and DPC induced in human promyelocytic leukemia HL-60 cells. Treatment of HL-60 cells with azatoxin produced both SSB and DPC. SSB were detected within 5 min of drug exposure, remained constant in number during treatment, and were reversed within 5 min after drug removal (Fig. 2). The DPC curve was superimposable with the SSB curve (Fig. 2), demonstrating a near 1:1 equivalence between SSB and DPC as expected for top2-mediated DNA breaks [4]. The lowest azatoxin concentration that produced detectable DNA damage was 5 μM, and DNA damage increased

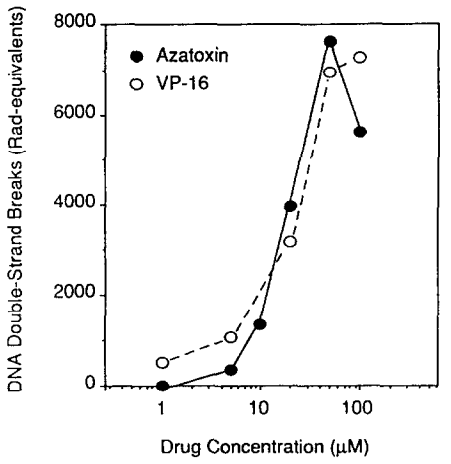

Fig. 3. DSB induced by azatoxin and VP-16 in HL-60 cells treated for 30 min. At the end of drug treatment, cells were washed twice in ice-cold drug-free medium and assayed by alkaline elution under DNA non-denaturing conditions. Each point represents an independent determination.

with drug concentration up to 100 μM (data not shown). The breaks were not detectable under non-deproteinizing conditions, which result in retention of protein-linked DNA fragments on the elution filter. These data are consistent with the induction of top2-linked DNA breaks by azatoxin in cells.

Azatoxin-induced DNA damage was quantitatively comparable to that induced by VP-16 (data not shown), indicating that azatoxin was approximately equipotent with VP-16 in HL-60 cells.

SSB induced by azatoxin in HL-60 cells. Typical top2-mediated DNA strand breakage is characterized by a large number of DSB [4]. Indeed, azatoxin-induced DSB were easily detectable by alkaline elution (Fig. 3). As in the case of SSB, the threshold concentration was between 5 and 10 μM, and DSB frequency was comparable to that obtained with identical concentrations of VP-16 (Fig. 3). Computation [8] of the SSB and DSB results shown on Figs. 2 and 3, respectively, yielded a ratio of true SSB per DSB of approximately 15 at 10 μM azatoxin, 4 at 20 μM, and 3 at 50 μM. Therefore, as with VP-16, azatoxin induces a mixture of true SSB and DSB and the ratio of SSB to DSB falls as the drug concentration rises [4].

Cytotoxicity of azatoxin. Azatoxin was tested in the *in vitro* NCI-Drug-Screen using 45 cell lines (see legend of Fig. 4) with standard 48-hr continuous drug exposures (Fig. 4). The mean azatoxin concentration producing 50% growth inhibition (GI_{50}) was 0.13 μM. The most sensitive cell lines were the 6 colon, 4 melanoma, 5 leukemia, and 2 small cell lung cancer lines. Among the most resistant cell lines, were 1 out of the 8 central nervous system lines (SNB-19), 1 out of the 5 renal cancer lines (SN12C), 3 out of the 10-non-small cell lung cancer lines (EKVX, HOP-18, and HOP-92), and 2 out of the 5 ovarian lines (OVCAR-4 and OVCAR-5).

Analysis of the data with the COMPARE algorithm [5, 16] revealed a poor correlation with other top2 inhibitors but a good correlation with tubulin inhibitors. Plots of 50% growth inhibitory concentrations of drug pairs (Fig. 4) show the good correlation of vinblastine versus azatoxin (correlation coefficient, $r^2 = 0.76$) (upper left panel), and the lack of correlation of VP-16 versus azatoxin ($r^2 = 0.31$) (lower left panel). The two right panels exemplify the even better correlations of VM-26 versus VP-16 ($r^2 = 0.90$) and of taxol versus vinblastine ($r^2 = 0.81$). These data suggested that azatoxin might be a tubulin inhibitor.

In addition, examination of the 48-hr exposure concentration–response curves for individual cell lines in the NCI-Drug-Screen revealed that for several cell lines cytotoxicity was maximum around 1 μM and was less pronounced at 10 μM. This unusual effect was investigated more closely in HL-60 and KM20L2 cells treated with azatoxin for various time periods (between 1 and 96 hr) (Fig. 5). At 0.1 and 1 μM, cytotoxicity was highly dependent upon drug exposure time. Treatment for at least 24 hr was highly cytotoxic, while 1- to 8-hr treatments with azatoxin were less effective. Interestingly, reduced cell loss was observed for drug exposures exceeding 24 hr at and above 10 μM azatoxin (Fig. 5).

Azatoxin cytotoxicity was examined further by colony-formation assays in KM20L2 cells (Fig. 6). After 24-hr treatments, 60–80% of the cells were detached from the plates at and above 0.5 μM azatoxin (panel A). Detached cells were observed to die rapidly by apoptosis (data not shown). The remaining attached cells were plated for colony-formation assay, and colonies were counted after 10–12 days (panel B). Plating efficiencies from control cells ranged from 40 to 65%. Azatoxin at 0.5 μM reduced survival to 30–50%, between 0.5 and 10 μM the survival rate remained flat, and between 10 and 100 μM cytotoxicity increased markedly (panel B). Since these data suggested a two-step cytotoxic effect, a composite graph was generated by multiplying the data of panels A and B (panel C). Altogether, the results of these experiments indicate that azatoxin-induced cytotoxicity exhibits three concentration-dependent phases: the first between 0.1 and 0.5 μM, which produces approximately 95% cell killing, the second between 0.5 and 10 μM where no further cytotoxicity occurs, and the third where cell killing increases sharply at azatoxin concentrations above 10 μM (Fig. 6C).

Tubulin polymerization inhibition by azatoxin. Evidence for an interaction of azatoxin with tubulin was obtained using a tubulin polymerization assay. Figure 7 shows a typical experiment in which tubulin polymerization was induced by a rapid increase of temperature from 0 to 30° and depolymerization by the reverse temperature change (arrow). Azatoxin inhibited tubulin polymerization and had no apparent effect on the kinetics of depolymerization. The concentration inhibiting the extent of polymerization by 50% (IC_{50}) after a 20-min incubation was 4.02 ± 0.05 μM (N = 3). Other antimitotic agents examined under identical reactions conditions have yielded

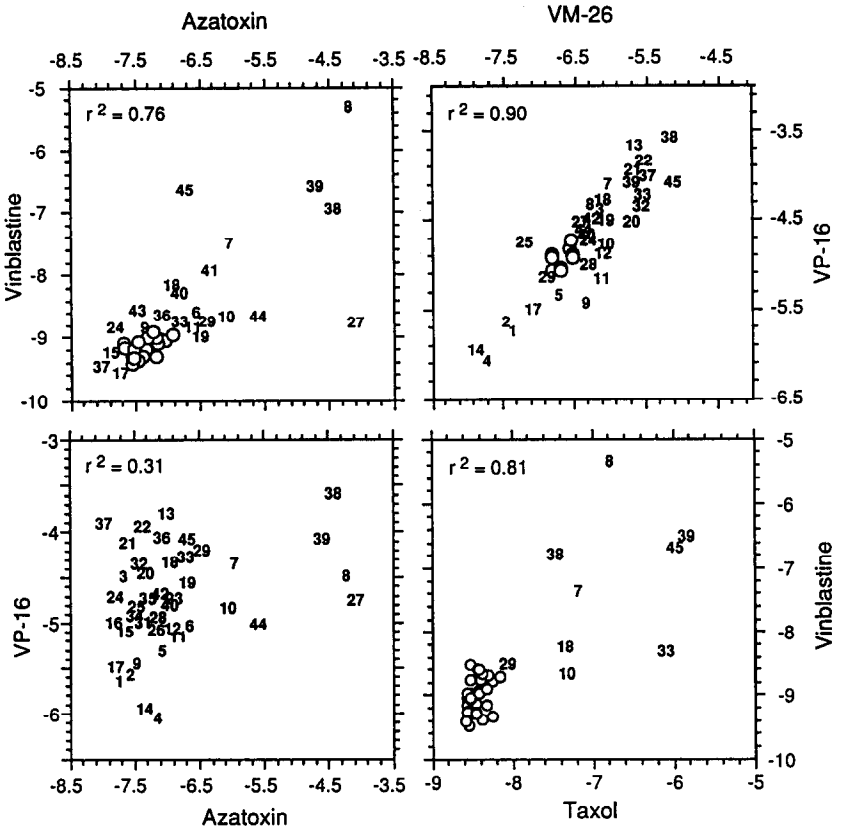

Fig. 4. Cytotoxicity of azatoxin in the NCI-Drug-Screen and correlations with vinblastine, VP-16, VM-26, and taxol. Numbers on the axes correspond to $\log(GI_{50})$, where GI_{50} is the drug concentration that inhibits cell growth by 50%. Correlation coefficients (r^2) are indicated for each graph. Numbers correspond to cell lines as follows: *leukemias:* 1: CCRF-CEM, 2: HL-60, 3: K562, 4: MOLT-4, and 5: RPMI-8226; *non-small cell lung cancers:* 6: A549, 7: EKVX, 8: HOP-18, 9: HOP-62, 10: HOP-92, 11: NCI-H226. 12: NCI-H23, 13: NCI-H322M, 14: NCI-H460, and 15: NCI-H522; *small cell lung cancers:* 16: DMS114, and 17: DMS273; *colon cancers:* 18: DLD-1, 19: HCC-2998; 20: HCT-116, 21: HT29, 22: KM20L2, and 23: SW-620; *central nervous system cancers:* 24: SF-268, 25: SF-295, 26: SF-539, 27: SNB-19, 28: SNB-75, 29: SNB-78, 30: U251, and 31: XF498; *melanomas:* 32: M19-MEL; 33: SK-MEL-28, 34: SK-MEL-5, and 35: UACC-62; *ovarian cancers:* 36: IGROV1, 37: OVCAR-3, 38: OVCAR-4, 39: OVCAR-5, and 40: OVCAR-8; *renal cancers:* 41: ACHN, 42: RXF-393, 43: RXF-631, 44: SN12C, and 45: UO-31. Numbers are replaced by circles in regions with overlapping numbers.

IC_{50} values as low as 0.64 μM (for thiocolchicine, an especially potent analog of colchicine [13]).

Azatoxin-induced tubulin and top2 inhibition in KM20L2 cells. Inhibition of cellular tubulin was investigated in KM20L2 cells treated with azatoxin for 24 hr (Fig. 8). Azatoxin produced a strong G_2/M block associated with an increase of mitotic index at 1 μM and above. Since the mitotic index was comparable to that induced by 0.2 μM colchicine, a classic mitotic inhibitor (data not shown), azatoxin appears to inhibit tubulin polymerization both *in vitro* and in cells.

Azatoxin-induced top2 inhibition was also investigated in KM20L2 cells by measuring drug-induced SSB (Fig. 9). The lowest concentration for which SSB were detectable was 10 μM, which is 10-fold higher than for the concentration required for G_2/M block and tubulin inhibition (see above). These results indicate that azatoxin is a dual inhibitor of tubulin and top2. At low concentrations, the main effect may be tubulin inhibition, while above 10 μM topoisomerase II also becomes inhibited.

DISCUSSION

The rationale for developing novel top2 inhibitors, such as azatoxin, is that top2 is the major target of a number of anticancer drugs, including the epipodophyllotoxins (VP-16 and teniposide [VM-26]), the anthracyclines (doxorubicin [Adriamycin®], 4'epidoxorubicin [Epirubicin®], daunorubicin, 4-demethoxydaunorubicin (Idarubicin®]), amsacrine, ellipticine and mitoxantrone. Top2 inhibition by these drugs and by azatoxin is due to the enzyme being trapped within cleavable complexes, which consist of DNA strand breaks covalently linked to top2 at their 5'-termini [2–4, 17, 18]. Top2 inhibitors that have varying spectra of anticancer activity do

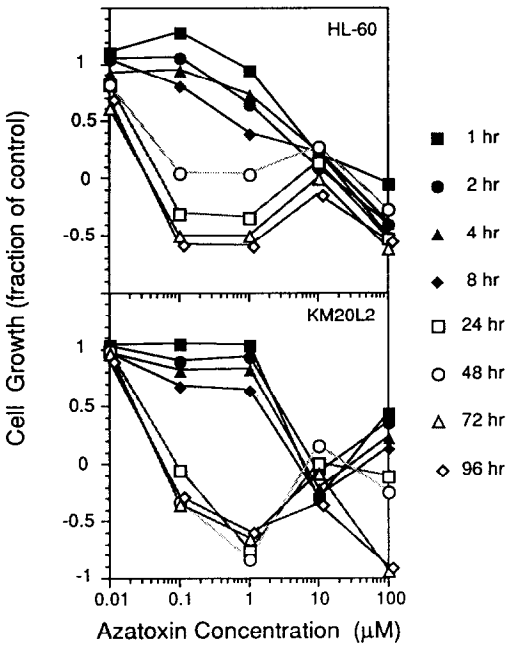

Fig. 5. Growth inhibitory effect of azatoxin in HL-60 and human colon carcinoma KM20L2 as a function of drug concentration and time. At the indicated times, azatoxin was removed by washing cell cultures twice in drug-free medium. Cells were allowed to grow for 48 hr. Growth inhibition was determined by the SRB assay (see Materials and Methods). Results of a typical experiment are shown.

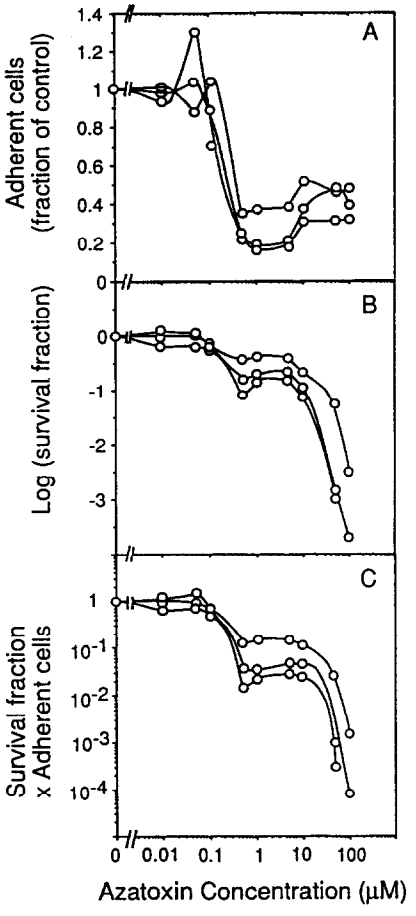

Fig. 6. Cytotoxicity of azatoxin as a function of drug concentration. Human colon carcinoma KM20L2 cells were plated for 24 hr, and then treated with azatoxin for 24 hr. At this time, cells that remained attached were counted and the fraction of detached cells was determined as compared with control cells (panel A). An equal number of attached cells were plated for the cloning assay, and colonies were counted after 10–12 days. Results are expressed as log (survival fraction) (panel B). Panel C was obtained by multiplying the data points of panels A and B in order to obtain a corrected log (survival fraction) taking into account the initial detachment of cells. Data from three independent experiments are shown in each panel.

differ from each other. First, the DNA sequence selectivity of top2 cleavage sites is different and specific for each class of drug [4, 17, 19–21]. Second, although most of these drugs are DNA intercalators, the epipodophyllotoxins and azatoxin lack this property [2, 4].

The present study shows that azatoxin induced protein-linked DNA breaks whose frequency was approximately equivalent to the frequency of azatoxin-induced DPC. These findings are consistent with induction of top2 cleavable complexes by azatoxin in two of the human cell lines that we have examined, promyelocytic leukemia HL-60 and colon cancer KM20L2. More breaks were produced in HL-60 cells than in KM20L2 cells and higher drug concentrations were required to induce similar break frequency in KM20L2 than in HL-60 cells, which is consistent with previous observations that HL-60 cells have relatively higher top2 levels than colon carcinoma cell lines [22].

Although VP-16 was slightly more potent at inhibiting top2 than azatoxin, azatoxin was markedly more cytotoxic than VP-16. The ratio of the VP-16 to azatoxin concentration producing 50% cell growth inhibition was 80 for HL-60 and 3000 for KM20L2 cells (Table 1). Although experimental conditions were different, results suggest a lack of correlation between protein-linked DNA break frequencies and cytotoxicity for azatoxin and VP-16. Similar discrepancies have been noticed previously when comparing top2 inhibitors from different chemical families [4]. However, in the case of azatoxin and VP-16, this discrepancy is particularly important, especially for the cell lines derived from solid tumors (Fig. 4). It is probably not explained by differences in cellular pharmacokinetics (drug uptake and egress from the cell), since kinetics of formation and reversal of protein-linked DNA breaks are rapid for both drugs (Fig. 3 and [23]). Moreover, the DNA sequence specificity differences of top2 cleavage sites induced by azatoxin and VP-16 were not as pronounced as in the case of VP-16 versus amsacrine or doxorubicin [2]. This suggests that the large difference in drug cytotoxicity is not due to this

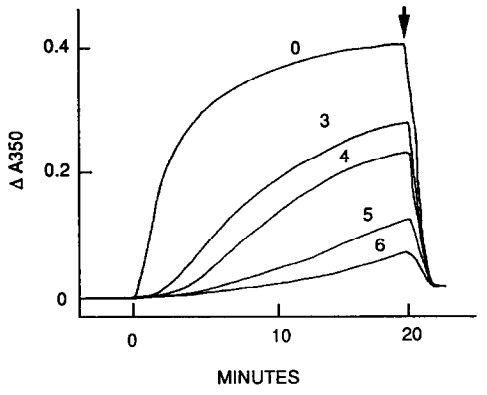

Fig. 7. Inhibition of tubulin polymerization by azatoxin. Polymerization was initiated by a rapid rise in temperature from 0 to 30° (about 60 sec). Time 0 was the point at which the reaction temperature reached 30°. Depolymerization was induced by a slower cooling of reaction mixtures to 0° (about 4 min) (arrow). Numbers above curves correspond to azatoxin concentrations (in μM).

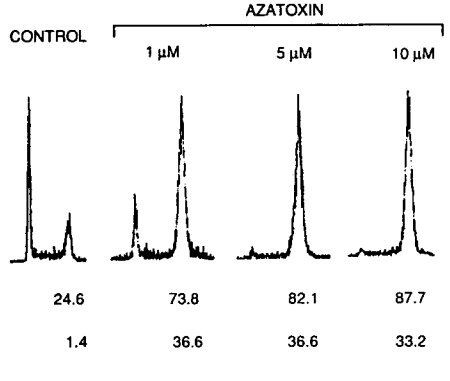

Fig. 8. Cell cycle alterations induced by azatoxin in KM20L2 cells. DNA content was analyzed using propidium iodide staining after 24-hr continuous treatments with azatoxin. Percentage of cells in G_2/M phase was computed using the SFIT model. Per cent of cells in mitosis was determined at the same times.

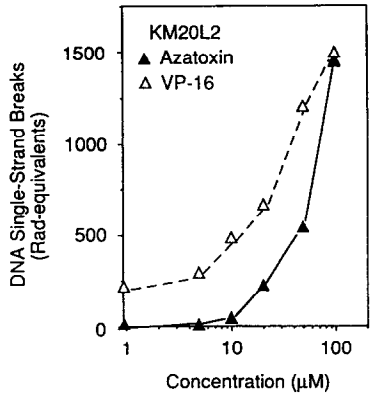

Fig. 9. Concentration–response curve of SSB induced by azatoxin in human colon carcinoma KM20L2 cells, and comparison with VP-16. After 30-min treatments, cells were washed twice in ice-cold drug-free medium and assayed by alkaline elution.

Table 1. Relationship between SSB and cytotoxicity for azatoxin and VP-16 in HL-60 and KM20L2 cells

	SSB 1000		GI_{50}	
	HL-60	KM20L2	HL-60	KM20L2
Azatoxin	15*	70	0.03	0.04
VP-16	15	35	2.4	120.2

* Numbers in the table are drug concentrations (in μM) required to induce either 1000 rad-equivalents SSB (1000) (approximately 1 break/10^6 nucleotides), or 50% cell growth inhibition (GI_{50}).

effect. Instead, it is more probable that the much greater potency of azatoxin relative to VP-16 derives from its antitubulin activity.

The antitubulin activity of azatoxin is interesting in view of the structure–activity relationship of tubulin inhibitors. The structure of azatoxin is very similar to that of 4′-demethyldeoxypodophyllotoxin [2], which is a potent tubulin polymerization inhibitor [24, 25]. Both compounds have the same dimethoxyphenol pendant ring and their global spatial configurations are almost superimposable [2]. Both compounds also bear a ketolactone group in corresponding regions. Moreover, dual inhibition of tubulin and top2 has also been found for demethylpodophyllotoxin derivatives [26]. The observations presented here demonstrate that the polycyclic ring system of podophyllotoxins can be changed without losing antitubulin or antitop2 activities. Since top2 inhibition by podophyllotoxin derivatives has been hypothesized to result from drug stacking within the DNA cleavage sites, it may be possible that tubulin bears a comparable drug-binding site [27].

Dual inhibition of top2 and tubulin by azatoxin appears to provide a potent cytotoxic compound that is active against solid tumors in the NCI cell screen. Top2 inhibitors were observed to induce G_2 block in colon cancer cells such as HT-29 [22] and KM20L2 cell (present study), whereas tubulin poisons induce arrest of the cell cycle in mitosis. A dual inhibitor of top2 and tubulin, such as azatoxin, would target the cell at two successive phases of the cell cycle. Those cells that escape the top2 inhibition-induced G_2 block could be stopped in mitosis and potentially die through the antitubulin activity of azatoxin.

REFERENCES

1. Macdonald TL, Lehnert EK, Loper JT, Chow K-C and Ross WE, On the mechanism of interaction of topoisomerase II with chemotherapeutic agents. In: *DNA Topoisomerases in Cancer* (Eds. Potmesil M and Kohn KW), pp. 199–214. Oxford University Press, New York, 1991.
2. Leteurtre F, Madalengoitia J, Orr A, Guzi TJ, Lehnert E, Macdonald T and Pommier Y, Rational design and molecular effects of a new topoisomerase II inhibitor, azatoxin. *Cancer Res* **52**: 4478–4483, 1992.

3. Liu LF, DNA topoisomerase poisons as antitumor drugs. *Annu Rev Biochem* **58**: 351–375, 1989.
4. Pommier Y and Kohn KW, Topoisomerase II inhibition by antitumor intercalators and demethylepipodophyllotoxins. In: *Developments in Cancer Chemotherapy* (Ed. Glazer RI), Vol. 2, pp. 175–196. CRC Press, Boca Raton, 1989.
5. Paull KD, Lin CM, Malspeis L and Hamel E, Identification of novel antimitotic agents acting at the tubulin level by computer-assisted evaluation of differential cytotoxicity data. *Cancer Res* **52**: 3282–3900, 1992.
6. Tomioka K, Kubota Y and Koga K, Synthesis and antitumor activity of podophyllotoxin aza-analogs. *Tetrahedron Lett* **30**: 2953–2954, 1989.
7. Kohn KW, Ewig RAG, Erickson LC and Zwelling LA, Measurement of strand breaks and crosslinks by alkaline elution. In: *DNA Repair: A Laboratory Manual of Research Procedures* (Eds. Friedberg EC and Hanawalt PC), pp. 379–401. Marcel Dekker, New York, 1981.
8. Zwelling LA, Michaels S, Erickson LC, Ungerleider RS, Nichols M and Kohn KW, Protein-associated deoxyribonucleic acid strand breaks in L1210 cells treated with the deoxyribonucleic acid intercalating agents 4′-(9-acridinylamino) methanesulfon-*m*-anisidide and adriamycin. *Biochemistry* **20**: 6553–6563, 1981.
9. Covey JM, Jaxel C, Kohn KW and Pommier Y, Protein-linked DNA strand breaks induced in mammalian cells by camptothecin, an inhibitor of topoisomerase I. *Cancer Res* **49**: 5016–5022, 1989.
10. Pommier Y, Schwartz RE, Kohn KW and Zwelling LA, Formation and rejoining of deoxyribonucleic acid double-strand breaks induced in isolated cell nuclei by antineoplastic intercalating agents. *Biochemistry* **23**: 3194–3201, 1984.
11. Monks A, Scudiero D, Skehan P, Shoemaker R, Paull K, Vistica D, Hose C, Langley J, Cronise P, Vaigro-Wolff A, Gray-Goodrich M, Campbell H, Mayo J and Boyd M, Feasibility of a high-flux anticancer drug screen using a diverse panel of cultured human tumor cell lines. *J Natl Cancer Inst* **83**: 757–766, 1991.
12. Pommier Y, Zwelling LA, Kao-Shan CS, Whang-Peng J and Bradley MO, Correlations between intercalator-induced DNA strand breaks and sister chromatid exchanges, mutations, and cytotoxicity in Chinese hamster cells. *Cancer Res* **45**: 3143–3149, 1985.
13. Getahun Z, Jurd L, Chu PS, Lin CM and Hamel E, Synthesis of alkoxy-substituted diaryl compounds and correlation of ring separation with inhibition of tubulin polymerization: Differential enhancement of inhibitory effects under suboptimal polymerization reaction conditions. *J Med Chem* **35**: 1058–1067, 1992.
14. Hamel E and Lin CM, Separation of active tubulin and microtubule-associated proteins by ultracentrifugation and isolation of a component causing the formation of microtubule bundles. *Biochemistry* **23**: 4173–4184, 1984.
15. Huang AB, Lin CM and Hamel E, Differential effects of magnesium on tubulin–nucleotide interactions. *Biochim Biophys Acta* **832**: 22–32, 1985.
16. Paull KD, Shoemaker RH, Hodes L, Monks A, Scudiero DA, Rubinstein L, Plowman J and Boyd MR, Display and analysis of patterns of differential activity of drugs against human tumor cell lines: Development of a mean graph and COMPARE algorithm. *J Natl Cancer Inst* **81**: 1088–1092, 1989.
17. Tewey KM, Rowe TC, Yang L, Halligan BD and Liu LF, Adriamycin-induced DNA damage mediated by mammalian DNA topoisomerase II. *Science* **226**: 466–468, 1984.
18. Capranico G, Zunino F, Kohn KW and Pommier Y, Sequence-selective topoisomerase II inhibition by anthracycline derivatives in SV40 DNA: Relationship with DNA affinity and cytotoxicity. *Biochemistry* **29**: 562–569, 1990.
19. Capranico G, Kohn KW and Pommier Y, Local sequence requirements for DNA cleavage by mammalian topoisomerase II in the presence of doxorubicin. *Nucleic Acids Res* **18**: 6611–6619, 1990.
20. Pommier Y, Capranico G, Orr A and Kohn KW, Distribution of topoisomerase II cleavage sites in SV40 DNA and the effects of drugs. *J Mol Biol* **222**: 909–924, 1991.
21. Pommier Y, Capranico G, Orr and Kohn KW, Local base sequence preferences for DNA cleavage by mammalian topoisomerase II in the presence of amsacrine and teniposide. *Nucleic Acids Res* **19**: 5973–5980, 1991.
22. Bertrand R, Sarang M, Jenkin J, Kerrigan D and Pommier Y, Differential induction of secondary fragmentation by topoisomerase II inhibitors in human tumor cell lines with amplified c-*myc* expression. *Cancer Res* **51**: 6280–6285, 1991.
23. Long BH, Musial ST and Brattain MG, Single- and double-strand DNA breakage and repair in human lung adenocarcinoma cells exposed to etoposide and teniposide. *Cancer Res* **45**: 3106–3112, 1985.
24. Kelleher JK, Tubulin binding affinities of podophyllotoxin and colchicine analogues. *Mol Pharmacol* **13**: 232–241, 1977.
25. Loike JD, Brewer CF, Sternlicht H, Gensler WJ and Horwitz SB, Structure–activity study of the inhibition of microtubule assembly *in vitro* by podophyllotoxin and its congeners. *Cancer Res* **38**: 2688–2693, 1978.
26. Liu Sy, Hwang BD, Haruna M, Imakura Y, Lee KH and Cheng YC, Podophyllotoxin analogs: Effects on DNA topoisomerase II, tubulin polymerization, human tumor KB cells, and their VP-16-resistant variants. *Mol Pharmacol* **36**: 78–82, 1989.
27. Hastie SB, Interactions of colchicine with tubulin. *Pharmacol Ther* **51**: 377–401, 1991.